Inhibited pattern formation by asymmetrical high-voltage excitation in nematic fluids

Péter Salamon, Nándor Éber, Balázs Fekete, and Ágnes Buka
Institute for Solid State Physics and Optics, Wigner Research Centre for Physics, Hungarian Academy of Sciences, H-1525 Budapest, P.O.B. 49, Hungary
(Received 15 June 2014; published 27 August 2014)

In contrast to the predictions of the standard theory of electroconvection (EC), our experiments showed that the action of superposed ac and dc voltages rather inhibits pattern formation than favors the emergence of instabilities; the patternless region may extend to much higher voltages than the individual ac or dc thresholds. The pattern formation induced by such asymmetrical voltage was explored in a nematic liquid crystal in a wide frequency range. The findings could be qualitatively explained for the conductive EC, but represent a challenging problem for the dielectric EC.

DOI: 10.1103/PhysRevE.90.022505 PACS number(s): 61.30.Gd, 47.54.−r

I. INTRODUCTION

Instabilities in nonlinear dynamical systems can lead to formation of patterns [1]. In fluids, patterns are often associated with vortex flow induced by various driving forces such as temperature gradient (Rayleigh-Bénard convection [2–5]), shear (Taylor-Couette flow [6–9], Kelvin-Helmholtz instability [10,11]), or electric field (electroconvection (EC) [12]). Anisotropic fluids are especially convenient to study some general features of dynamical systems, as they are prone to show easily observable convective patterns in applied electric fields because of their optical anisotropy.

Electroconvection in nematic liquid crystals [12] can be induced by both direct (dc) and alternating (ac) voltages in the same compound. In this paper, we show that the application of asymmetrical voltages corresponding to the superposition of a dc and a sinusoidal ac signal can inhibit the formation of patterns, even if the ac and dc components are an order of magnitude higher than the threshold voltages of the purely ac- or purely dc-induced electroconvection.

Nematic liquid crystals are mostly composed of elongated molecules with their long molecular axes fluctuating around an average direction, the director $\mathbf{n}(\mathbf{r})$ [13]. Due to their uniaxial symmetry, nematic materials can be characterized by two independent dielectric constants measured with electric fields parallel or perpendicular to the director ($\varepsilon_{||}$ and $\varepsilon_{\perp}$, respectively). A positive or negative dielectric anisotropy $\varepsilon_a = \varepsilon_{||} - \varepsilon_{\perp}$ allows one to align the director parallel with or perpendicular to the electric field, respectively [13].

Liquid crystals are studied and used mostly in thin (5–20 μm) films, sandwiched between glass plates with transparent electrodes providing an electric field along the cell normal. A proper treatment can ensure strongly anchored, homogeneous director alignment at the surfaces. In a planar cell, the homogeneous director lies in the cell plane. Due to the electric field applied perpendicular to the initial director, if $\varepsilon_a > 0$, an instability occurs at a critical voltage U_{cF} leading to a homogeneous director deformation, called the Freedericksz transition.

The electric Freedericksz transition can be induced by dc ($U_{\rm dc}$) as well as by sinusoidal ac ($U_{\rm ac}$) voltages of frequency f [14]. In the case of an asymmetrical driving, the applied voltage is described by $U = U_{\rm dc} + \sqrt{2}U_{\rm ac}\sin(2\pi f t)$. The onset of the instability can be achieved by different combinations of the two control parameters, $U_{\rm dc}$ and $U_{\rm ac}$, characterized by a frequency-independent threshold curve: a quarter circle in the $U_{\rm ac}$-$U_{\rm dc}$ plane given by $U_{cF}^2 = U_{\rm dc}^2 + U_{\rm ac}^2$. Inside this curve the system is in its homogeneous basic state; outside the initial planar state is deformed.

If $\varepsilon_a < 0$, the electric field exerts a stabilizing torque on the director, however, an instability can still take place leading to a periodic director deformation by convection, governed mostly by the Carr-Helfrich mechanism: Spatial director fluctuations lead to space charge separation due to the conductivity anisotropy $\sigma_a = \sigma_{||} - \sigma_{\perp}$ ($\sigma_{||}$ and $\sigma_{\perp}$ are the conductivities measured with an electric field parallel and perpendicular to the director, respectively); the Coulomb force induces flow forming vortices due to the constraining surfaces; the flow exerts a destabilizing torque on the director [12]. Above a critical voltage U_c, the fluctuations do not decay, but grow to a macroscopic pattern of convection rolls characterized by a critical wave vector $\mathbf{q_c}$. The typical case of electroconvection (standard EC) can be observed in a planar cell filled with a nematic liquid crystal with $\varepsilon_a < 0$ and $\sigma_a > 0$. The resulting patterns correspond to a spatially periodic system of convection rolls that appear as dark and bright stripes perpendicular (or oblique) to the initial director in a microscope.

Different modes of EC can be realized at the onset of the instability depending on the frequency. Typically at high f, the *dielectric mode* is present; then by decreasing f, a transition to the *conductive mode* occurs at the crossover frequency f_c [12]. In cells of typical thickness, this transition is easily observable due to the largely different $\mathbf{q_c}$ of the two modes.

A comprehensive theoretical description of the different pattern forming modes in nematic liquid crystals is provided by the so-called standard model of EC (SM) [15], which has recently been improved by including flexo-electricity (extended SM) [16]. It combines the equations of nematohydrodynamics with those of electrodynamics, while assuming ohmic electrical conductivity. The extended SM provides $U_c(f)$, $\mathbf{q}_c(f)$, and the spatio-temporal dependence of the director $\mathbf{n}(\mathbf{r},t)$ at onset, in agreement with experiments. For EC, the equations exhibit solutions with three different time symmetries. One is found at dc driving, where $\mathbf{n}(\mathbf{r})$, the flow field $\mathbf{v}(\mathbf{r})$, and the charge field $\varrho_e(\mathbf{r})$ are static. The other two occur at ac voltage excitation: In the conductive mode, the director and the flow is stationary in leading order (if f is

much larger than the inverse director relaxation time τ_d^{-1}), so the time average of the director tilt over the driving period is nonzero ($\langle n_z(t)\rangle \neq 0$) while space charges oscillate with f; in the dielectric mode, $\varrho_e(\mathbf{r})$ is stationary while $\mathbf{n}(\mathbf{r})$ and $\mathbf{v}(\mathbf{r})$ oscillate with f (thus $\langle n_z(t)\rangle = 0$).

Pattern formation may also occur at superposing two electric signals. The behavior of EC has been studied at adding sinusoidal or square wave voltages of two distinct frequencies ($f_1 < f_2$, f_2 being a multiple of f_1) and a nontrivial threshold variation and a reentrant pattern forming behavior was found [17,18]. Here we report on the mostly unexplored case of superposing ac and dc voltages. As standard EC may occur at pure dc as well as at pure ac excitation, one might expect it to arise at a combined, asymmetrical driving, too, just like in the case of the electric Freedericksz transition. We raised the questions, how this nonlinear dynamical system responds to the asymmetric excitation and which kind of pattern morphologies will occur. The consequences of the asymmetric driving in standard EC are mostly unexplored experimentally and are challenging also from the theoretical point of view; the solution may not be obtained as a simple superposition of the three modes of different time symmetries mentioned above. Recent studies have shown that the extended SM can well describe the limits of stability in the $U_{ac} - U_{dc}$ plane for the conductive EC if f is sufficiently low ($f \ll f_c$); then the threshold curve is similar to that of the Freedericksz transition [19]. Our present experimental work aimed to provide a more comprehensive study on a broad range of f. It will be shown that the onset behavior of the system is qualitatively different depending on the frequency.

II. EXPERIMENTAL

Our experiments were carried out using the nematic mixture Phase 5. It exhibits $\varepsilon_a < 0$ and $\sigma_a > 0$ and is a widely used material for studying standard EC [20]. When applying ac voltage driving, depending on f, both dielectric and conductive EC can be observed. We used $d = 10.8$ μm thick cells (E.H.C. Co., Japan) at the temperature of $T = 30 \pm 0.05\,^{\circ}$C for the measurements. Applying dc voltage, our planar samples showed EC. The patterns were observed in a polarizing microscope using the shadowgraph technique [21–23]; the EC thresholds were determined in the $U_{ac} - U_{dc}$ plane at different frequencies of the ac signal. The searching for patterns was done at a fixed ac voltage varying the dc component.

III. RESULTS AND DISCUSSION

In Fig. 1, the threshold curves showing the limits of stability in the $U_{ac} - U_{dc}$ plane are presented for $f = 400$ Hz. They exhibit a strikingly different behavior compared to the quarter circle of the Freedericksz transition. The threshold curves starting from $U_{dc} = 0$ V and $U_{ac} = 0$ V form two branches (the ac and dc branches, respectively), which do not cross each other in the available voltage range. At $U_{dc} = 0$ V, $U_{ac} \gtrsim 24$ V, regular dielectric EC rolls are seen that lie normal to the initial director. Following the threshold curve on the ac branch, the morphology remains the same, but surprisingly, with increasing U_{dc} along the curve, U_{ac} also becomes higher; the curve bends away from the origin towards higher U_{ac},

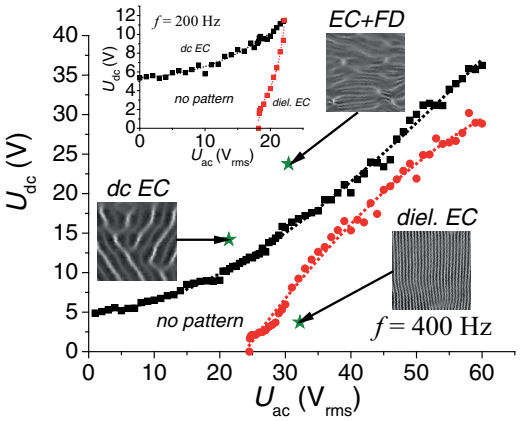

FIG. 1. (Color online) Morphological phase diagram of a Phase 5 sample at $f = 400$ Hz, and at $f = 200$ Hz (inset from [19]). The dashed lines, as a guide for the eyes, indicate the trends of the stability limit curve. Stars indicate those U_{ac}, U_{dc} combinations where the images covering an area of 52 μm × 52 μm were taken. The initial director lies along the horizontal direction.

U_{dc} values. If $U_{ac} = 0$ V, dc EC can be observed as a roll structure oblique to the initial director. Following the threshold curve on this dc branch, with increasing U_{ac} EC appears at higher U_{dc}, and the slope remains positive. We note that at $U_{dc} > 23$ V, besides EC, stripes parallel to the director also appear in patches; they are attributed to flexoelectric domains (FDs [20,24–27]).

The two branches of the stability limit in Fig. 1 correspond to patterns with different morphologies and significantly different wave numbers. In the narrow channel between the two branches no patterns could be detected. Surprisingly, the system remains there in the basic, undistorted state despite the high voltages applied. For example, at $U_{dc} = 32$ V and $U_{ac} = 55$ V, the dc and ac voltage components are more than 6 and 2 times larger than the corresponding thresholds for purely dc and purely ac driving, respectively. In the case of purely ac or dc driven EC, at voltages so much above the thresholds, the convection would already be in the turbulent regime. Our findings thus indicate that using a signal with properly adjusted asymmetry can result not only in the suppression of undesirable turbulence but also in complete inhibition of pattern formation. An unusual sequence of morphologies can be obtained by varying one voltage component while the other is kept constant. For example, at fixed $U_{ac} = 40$ V, with no dc component, the convection is turbulent. Increasing U_{dc}, the system behaves less and less overdriven; it shows regular patterns at $U_{dc} \approx 16$ V, then if 16 V $\lesssim U_{dc} \lesssim 20$ V, there is no pattern at all. Applying higher U_{dc}, electroconvection sets in again, and becomes turbulent at high values of U_{dc}.

The inhibition of pattern formation at combined ac and dc driving holds also at higher frequencies. Decreasing f, however, leads to a qualitatively different behavior. At $f =$ 200 Hz (inset in Fig. 1), the pattern morphologies in the $U_{ac} - U_{dc}$ plane at onset are similar, but now the ac and dc branches cross each other; the pattern-free channel closes at some voltages, where a morphological transition occurs between the conductive and dielectric roll structures [19].

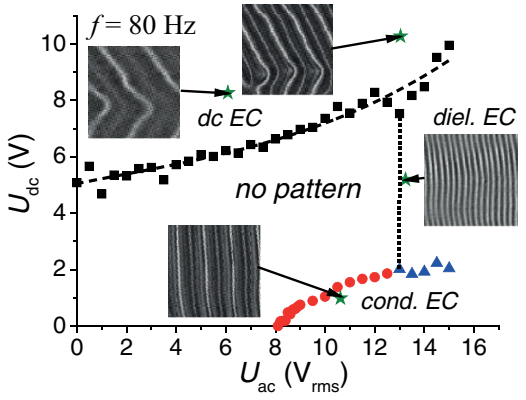

FIG. 2. (Color online) Morphological phase diagram of a Phase 5 sample at $f = 80$ Hz. The dashed lines, as a guide for the eyes, indicate the trends of the stability limit curve. The dotted line shows the boundary between the patternless basic state and the region of dielectric electroconvection. Stars indicate those U_{ac}, U_{dc} combinations where the images covering an area of 52 μm × 52 μm were taken. The initial director lies along the horizontal direction.

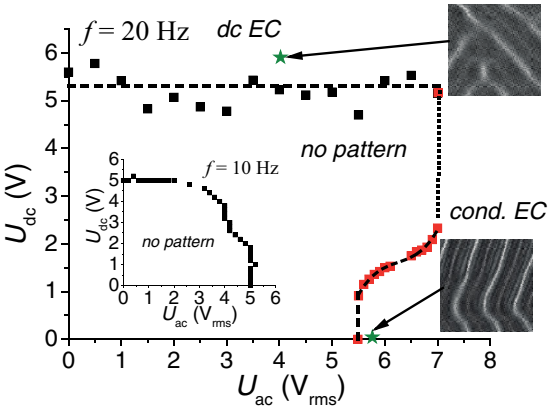

FIG. 3. (Color online) Morphological phase diagram of a Phase 5 sample at $f = 20$ Hz, and at $f = 10$ Hz (inset from [19]). The dashed lines, as a guide for the eyes, indicate the trends of the stability limit curve. The dotted line shows the boundary between the patternless basic state and the region of conductive electroconvection. Stars indicate those U_{ac}, U_{dc} combinations where the images covering an area of 52 μm × 52 μm were taken. The initial director lies along the horizontal direction.

The purely ac driving at $f = 80$ Hz yields conductive EC. The ac branch of the stability limit curve in Fig. 2 exhibits a positive slope in the U_{ac}-U_{dc} plane until $U_{dc} = 2$ V, where the conductive roll structure crosses over to the dielectric one, indicated by a large increase of the wave number. At this morphological transition, the slope of the curve also changes abruptly: For dc voltages $U_{dc} > 2$ V the threshold curve is characterized by an unaltered U_{ac} component until the crossing with the dc branch (see dotted line in Fig. 2). There an additional morphological transition occurs between the dielectric and the dc EC modes, shown again by a significant change in the wave number.

At even lower frequencies, a dc-voltage-induced transition to the dielectric EC does not occur; as a consequence there is no dramatic change in the critical wave number along the stability limit curve in the U_{ac}-U_{dc} plane. Nevertheless, depending on the frequency, the system can show different characteristics. At $f = 20$ Hz (see Fig. 3), the ac branch shows mainly a positive slope that results in a larger pattern-free area compared to the expected quarter-ellipse-shaped threshold curve, found earlier at $f = 10$ Hz [19] (see inset in Fig. 3).

Recently, the critical voltages and wave numbers were calculated at the onset of EC induced by superposed ac and dc voltages [19]. Both analytical and numerical calculations predicted that the dc branch has positive slope in the U_{ac}-U_{dc} plane at higher frequencies and negative slope at lower frequencies. This is in good agreement with the experimental data in Figs. 1–3. The theoretical work also pointed out that the ac branch should exhibit negative slope if $U_{dc} > 0$ V, for the conductive as well as for the dielectric modes. The experiments confirmed this behavior for the conductive EC, however, for the lowest frequency only (inset in Fig. 3).

For higher frequencies in the conductive EC range ($f = 20$ Hz or $f = 80$ Hz), in contrast to the theoretical expectation, the slope of the ac branch was experimentally found positive; i.e., in the presence of a dc bias the EC instability sets in at higher U_{ac} values. The standard model of EC, which assumes constant ohmic conductivity, cannot account for this finding. One should note, however, that assuming a voltage-independent (ohmic) conductivity in the case of a weak electrolyte, such as a liquid crystal, is not always realistic. If the applied ac voltage is not symmetric, i.e., a nonzero dc component is present, the number of effective charge carriers may decrease, because a fraction of ions is immobilized at the electrodes coated with insulating (polyimide) surfaces. Therefore the bulk conductivity of the liquid crystal is expected to decrease with increasing U_{dc}; this was actually verified by simultaneous conductivity measurements. Consequently, during the experiments shown in Figs. 1–3 the conductivity changes from point to point in the U_{ac}-U_{dc} plane, in contrast to the constant σ value assumed in the theoretical calculations [19].

In the case of the purely ac driven conductive EC, the threshold voltage at a fixed frequency increases if the conductivity is reduced [12,28]. This increment is larger at higher frequencies, being closer to the conductive-dielectric crossover. This behavior offers a qualitative explanation to the shape mismatch between the expected and measured stability limit curves in the conductive regime. Application of U_{dc} results in lowering the conductivity, which leads to a higher onset U_{ac} of EC than expected for a constant σ. The higher the frequency, the more probable that this threshold increment flips the slope of the ac branch from negative to positive, as found in Figs. 2 and 3. Lowering the conductivity by the dc bias reduces the crossover frequency f_c as well. If due to this reduction f_c becomes lower than the driving frequency, a dc-voltage-induced transition from the conductive to the dielectric mode occurs, as was actually found at $f = 80$ Hz (Fig. 2).

Understanding the characteristics of the dielectric EC at an asymmetric voltage driving is more challenging. On the one hand, calculations have shown that the ac and dc branches of the stability limit curve do not connect smoothly, as there is a sharp change in the critical wave number [19]; these features were confirmed by the experiments at lower

frequencies in the dielectric regime (inset in Fig. 1). On the other hand, a discrepancy exists, since in contrast to the theory, the experimental slope of the ac branch is positive. The dc-voltage-induced σ reduction (which was a clue for the conductive EC) does not help here; in the case of dielectric EC the theory predicts diminishing ac threshold voltages for a lower conductivity. Consequently, when increasing U_{dc}, the U_{ac} component at the onset of the instability is expected to be even smaller than without considering the change in the conductivity, while experiments show U_{ac} increasing with U_{dc}. Moreover, this increment becomes larger at higher frequencies, leading finally to the inhibition of pattern formation, i.e., the extension of the stability limit to such U_{ac}, U_{dc} voltage components that are several times higher than the threshold voltages at purely ac or purely dc voltage excitation (see the channel in Fig. 1).

The (extended) standard model of EC is not able to account for the inhibited pattern formation and for the dramatic effect of the frequency on the onset characteristics of the dielectric EC at asymmetrical voltage driving.

However unexpected the inhibition of electroconvective pattern formation shown above is, it is not fully unprecedented. A much less pronounced inhibition has already been reported earlier [17,18] for samples driven by a superposition of harmonic or square waves, with frequency ratios of a small integer number, i.e., by signals with the same time symmetries. In that case the pattern-free region could be extended only by a few percent of the higher f ac voltage, in contrast to the huge increment shown in Fig. 1.

We anticipate that ionic effects originating in the electrolytic nature of liquid crystals, such as voltage-dependent conductivity (electropurification), internal voltage attenuation in the cell, and Debye layers at the boundaries may play an important role. Some earlier reports indicated that the dielectric EC rolls are rather localized at the cell surfaces than in the bulk [29,30]. Taking into account that significant electric field gradients may exist on the length scale of the dielectric rolls in the vicinity of the electrodes, this might account for why the behavior of dielectric EC is more anomalous than the conductive EC.

In order to include the above-mentioned effects and therefore to give a more complete explanation of our findings, the basic assumption of the (extended) SM on the ohmic conductivity should be given up. A weak electrolyte model (WEM), accounting for ionic dissociation-recombination processes, was developed more than a decade ago [31–34]. The WEM introduced additional variables (the ionic concentrations) with rate equations with two additional time scales (for the recombination and migration times of ions), and with the relevant (mostly unknown) material parameters (e.g., ionic mobilities). The resulting set of partial differential equations, which is even more complex than that of the extended SM, has only partially been analyzed to prove the ionic origin of the Hopf bifurcation (traveling waves) in ac-driven EC. We expect that the WEM, generalized with the inclusion of flexoelectric phenomena, would be a proper theoretical tool to describe the dc-voltage-induced phenomena, including the inhibition of the pattern formation. Such an analysis is, however, a huge theoretical challenge for the future.

IV. CONCLUSIONS

In summary, we reported convective pattern formation in a nematic fluid induced by asymmetric voltage signals, exhibiting a rich variety of morphological transitions. The experiments showed, in contrast to our intuition and the predictions of the (extended) standard model of EC, that the joint action of ac and dc voltages rather inhibits pattern formation than favors the emergence of instabilities. While for the conductive EC a qualitative explanation based on the change of conductivity could be given, the question of why the pattern formation is largely inhibited in the dielectric mode at high frequencies still needs to be precisely answered in the future. The unexpected suppression of pattern formation at high applied voltages can open new horizons in studies of (sub)criticality or director fluctuations in electric fields in voltage ranges where investigations were believed to be impossible due to the occurrence of patterns or turbulent flow of the material. Our finding also raises the question whether analogous effects can be found in other dynamical systems, such as isotropic EC, or shear induced turbulent convection combined by electric fields.

ACKNOWLEDGMENTS

Financial support from the Hungarian Research Fund (Grants No. OTKA K81250 and No. NN110672) are gratefully acknowledged. The authors are grateful to Werner Pesch and Alexei Krekhov for fruitful discussions.

[1] M. C. Cross and P. C. Hohenberg, Rev. Mod. Phys. **65**, 851 (1993).
[2] G. Ahlers, S. Grossmann, and D. Lohse, Rev. Mod. Phys. **81**, 503 (2009).
[3] G. Ahlers, E. Bodenschatz, D. Funfschilling, S. Grossmann, X. He, D. Lohse, R. J. A. M. Stevens, and R. Verzicco, Phys. Rev. Lett. **109**, 114501 (2012).
[4] K. Petschel, S. Stellmach, M. Wilczek, J. Lülff, and U. Hansen, Phys. Rev. Lett. **110**, 114502 (2013).
[5] R. du Puits, L. Li, C. Resagk, A. Thess, and C. Willert, Phys. Rev. Lett. **112**, 124301 (2014).
[6] S. G. Huisman, D. P. M. van Gils, S. Grossmann, C. Sun, and D. Lohse, Phys. Rev. Lett. **108**, 024501 (2012).
[7] Y. Duguet and P. Schlatter, Phys. Rev. Lett. **110**, 034502 (2013).
[8] S. G. Huisman, S. Scharnowski, C. Cierpka, C. J. Kähler, D. Lohse, and C. Sun, Phys. Rev. Lett. **110**, 264501 (2013).
[9] K. Deguchi, A. Meseguer, and F. Mellibovsky, Phys. Rev. Lett. **112**, 184502 (2014).
[10] Y. Kuramitsu, Y. Sakawa, S. Dono, C. D. Gregory, S. A. Pikuz, B. Loupias, M. Koenig, J. N. Waugh, N. Woolsey, T. Morita, T. Moritaka, T. Sano, Y. Matsumoto, A. Mizuta, N. Ohnishi, and H. Takabe, Phys. Rev. Lett. **108**, 195004 (2012).

[11] O. A. Hurricane, V. A. Smalyuk, K. Raman, O. Schilling, J. F. Hansen, G. Langstaff, D. Martinez, H.-S. Park, B. A. Remington, H. F. Robey, J. A. Greenough, R. Wallace, C. A. Di Stefano, R. P. Drake, D. Marion, C. M. Krauland, and C. C. Kuranz, Phys. Rev. Lett. **109**, 155004 (2012).
[12] L. Kramer and W. Pesch, in *Pattern Formation in Liquid Crystals*, edited by Á. Buka and L. Kramer (Springer-Verlag, New York, 1996), pp. 221–255.
[13] P. G. de Gennes and J. Prost, *The Physics of Liquid Crystals* (Oxford Science Publications, Oxford, 2001).
[14] I. Stewart, *The Static and Dynamic Continuum Theory of Liquid Crystals* (Taylor & Francis, New York, 2004).
[15] E. Bodenschatz, W. Zimmermann, and L. Kramer, J. Phys. (France) **49**, 1875 (1988).
[16] A. Krekhov, W. Pesch, N. Éber, T. Tóth-Katona, and Á. Buka, Phys. Rev. E **77**, 021705 (2008).
[17] J. Heuer, T. John, and R. Stannarius, Mol. Cryst. Liq. Cryst. **449**, 11 (2006).
[18] D. Pietschmann, T. John, and R. Stannarius, Phys. Rev. E **82**, 046215 (2010).
[19] A. Krekhov, W. Decker, W. Pesch, N. Éber, P. Salamon, B. Fekete, and Á. Buka, Phys. Rev. E **89**, 052507 (2014).
[20] N. Éber, L. O. Palomares, P. Salamon, A. Krekhov and Á. Buka, Phys. Rev. E **86**, 021702 (2012).
[21] S. Rasenat, G. Hartung, B. L. Winkler, and I. Rehberg, Exp. Fluids **7**, 412 (1989).
[22] S. P. Trainoff and D. S. Cannell, Phys. Fluids **14**, 1340 (2002).
[23] W. Pesch and A. Krekhov, Phys. Rev. E **87**, 052504 (2013).
[24] Y. P. Bobylev and S. Pikin, Zh. Eksp. Teor. Fiz. **72**, 369 (1977).
[25] A. Krekhov, W. Pesch, and Á. Buka, Phys. Rev. E **83**, 051706 (2011).
[26] P. Salamon, N. Éber, A. Krekhov, and Á. Buka, Phys. Rev. E **87**, 032505 (2013).
[27] Á. Buka and N. Éber, *Flexoelectricity in Liquid Crystals. Theory, Experiments and Applications* (Imperial College Press, London, 2012).
[28] W. Pesch and A. Krekhov (private communication).
[29] N. Gheorghiu, I. I. Smalyukh, O. D. Lavrentovich, and J. T. Gleeson, Phys. Rev. E **74**, 041702 (2006).
[30] H. Bohatsch and R. Stannarius, Phys. Rev. E **60**, 5591 (1999).
[31] M. Treiber and L. Kramer, Mol. Cryst. Liq. Cryst. **261**, 311 (1995).
[32] M. Dennin, M. Treiber, L. Kramer, G. Ahlers, and D. S. Cannell, Phys. Rev. Lett. **76**, 319 (1996).
[33] M. Treiber, N. Éber, Á. Buka, and L. Kramer, J. Phys. II (France) **7**, 649 (1997).
[34] M. Treiber and L. Kramer, Phys. Rev. E **58**, 1973 (1998).